Vol. 20, n.° 4, pp. 127-134, 2021
Revista UIS Ingenierías
Journal homepage: https://revistas.uis.edu.co/index.php/revistauisingenierias

A study of the structural, magnetic, and electrical properties of $Ba_{1-x}Na_xCoO_3$ compounds (x = 0.25, 0.5, 0.75)

Un estudio de las propiedades estructurales, magnéticas y eléctricas de los compuestos $Ba_{1-x}Na_xCoO_3$(x = 0.25, 0.5, 0.75)

Carlos A. Estrada-Rodríguez [1a], Lutiene Fernandes-Lopes [2a], Rovan Fernandes-Lopes [2b], Fabiano Mesquita [2c], Águeda M. Turatti [3a], Jorge L. Pimentel-Junior [3b], Santiago Sandoval-Gutiérrez [4], Carlos A. Parra-Vargas [1b]

[1] Grupo de Física de Materiales, Facultad de Ciencias, Universidad Pedagógica y Tecnológica de Colombia, Colombia. Emails: [a] caer8123@hotmail.com, [b] carlos.parra@uptc.edu.co. Orcid: [a] 0000-0003-3703-0708, [b] 0000-0001-8582-3337.
[2] Instituto de Física, Universidade Federal do Rio Grande do Sul, Brazil. Emails: [a] lutienefl@gmail.com, [b] rovanfl@gmail.com, [c] fabiano.mesquita@ufrgs.br. Orcid: [a] 0000-0002-5003-6330, [b] 0000-0002-3650-3983, [c] 0000-0002-2176-6975.
[3] Instituto de Física e Matemática, Universidade Federal do Rio Grande do Sul, Brazil. Emails: [a] amturatti@furg.br, [b] jorge@furg.br. Orcid: [a] 0000-0002-4732-8244, [b] 0000-0003-0968-0834,
[4] Grupo de Sistemas Dinámicos, Universidad de los Llanos, Villavicencio, Colombia. Email: samos16@gmail.com Orcid: 0000-0002-0680-606X.

Received: 12 November 2020. Accepted: 8 May 2021. Final version: 5 July 2021.

Abstract

Cobaltite-like materials having metal-insulator transitions are relevant in the consumer electronics market. In this work, we present the structural, magnetic, and electrical properties of $Ba_{1-x}Na_xCoO_3$ (with $x = 0.25, 0.5, 0.75$) cobaltite. All samples were synthesized using a solid-state reaction process. Their crystal structure was determined using X-ray diffraction (XRD) data by the Rietveld method, which showed that all the samples were crystallized in the orthorhombic space group C_{2221} (N.° 20). The microstructure of the sintered samples was characterized by scanning electron microscopy (SEM). The magnetic susceptibility measurements confirmed a paramagnetic behavior for $x \geq 0.5$ in the temperature range that was used. Likewise, a broad peak around *33 K* in the sample $x = 0.25$, and characteristic of antiferromagnetic behaviors were observed. On the other hand, resistivity contributed to determining the insulating behavior of samples where $x = 0.5$ and $x = 0.75$. In contrast, at low sodium content ($x = 0.25$), a metal-insulator transition was observed with transition temperature near *105 K*.

Keywords: X-ray diffraction; paramagnetic; order magnetic; metal-insulator transition; resistivity.

Resumen

Los materiales de tipo cobaltita que presentan transición metal-aislante tienen relevancia en el mercado de la electrónica de consumo. En este trabajo presentamos las propiedades estructurales, magnéticas y eléctricas de las cobaltitas $Ba_{1-x}Na_xCoO_3$ (con $x = 0.25, 0.5, 0.75$). Todas las muestras se sintetizaron mediante un proceso de reacción

ISSN Printed: 1657 - 4583, ISSN Online: 2145 - 8456,
How to cite: C. A. Estrada-Rodríguez, L. Fernandes-Lopes, R. Fernandes-Lopes, F. Mesquita, Á. M. Turatti, J. L. Pimentel-Junior, S. Sandoval-Gutiérrez, C. A. Parra-Vargas, "A study of the structural, magnetic, and electrical properties of $Ba_{1-x}Na_xCoO_3$ compounds (x = 0.25, 0.5, 0.75)," *Rev. UIS Ing.*, vol. 20, no. 4, pp. 127-134, 2021, doi: 10.18273/revuin.v20n4-2021010.

en estado sólido y su estructura cristalina se determinó a partir de datos de difracción de rayos X (DRX), mediante el método de Rietveld, el cual indicó que las muestras cristalizan en el grupo espacial ortorrómbico C_{2221} (N.º 20). La microestructura de las muestras sinterizadas se caracterizó mediante microscopía electrónica de barrido (MEB). Las medidas de susceptibilidad magnética confirmaron un comportamiento paramagnético para $x \geq 0.5$ en el rango de temperatura estudiado y un pico amplio alrededor de *33 K* en la muestra $x = 0.25$, lo cual es característico de los comportamientos antiferromagnéticos. Las medidas de resistividad permitieron determinar el comportamiento aislante de muestras con $x = 0.5$ y $x = 0.75$, mientras que a bajo contenido de sodio ($x = 0.25$), se observó una transición metal-aislante con temperatura de transición cercana a *105 K*.

Palabras clave: difracción de rayos X; paramagnético; orden magnético; transición metal-aislante; resistividad.

1. Introduction

In recent years, cobaltite Na_xCoO_2 materials have shown interesting physical properties, the phase diagrams of this system show electronic interactions evidencing some changes in sodium concentration [1]. Previous research has reported that an unusual charge of the ordering occurs at low concentrations, generated by two different magnetic states. These materials exhibited paramagnetic and metallic behaviors at low sodium concentration ($x < 0.5$), and a Curie-Weiss behavior at higher sodium concentration ($x > 0.5$) [1]. The cobaltite-type materials with the general formula $RECoO_3$ (RE = *La, Nd, Gd, Ho, Y*) have a crystal structure with rhombohedral symmetry at room temperature, where it changes in concentration generating structural distortions. Additionally, these systems show a semiconductor-metal transition at high temperatures [2].

Lanthanum cobaltite ($LaCoO_3$) has a magnetic behavior that is notably different due to spin-state transitions at *100* and *500 K*. In the latter temperature, a metal-insulator transition is evident as well [3]. Ren et al., who studied the praseodymium cobaltite, also observed an unusual spin transition [4]. The $La_{1-x}R_xCoO_3$ (R = Pr, Ca) system is of great interest due to the presence of a metal-insulator transition and the variability of magnetic and electrical properties with changes in the composition and temperature. The $La_{1-x}Ca_xCoO_3$ system exhibit a semiconductor behavior with $x \leq 0.15$, and metallic behavior in the concentration range *0.2-0.5* [5].

On the other hand, in the $La_{1-x}Pr_xCoO_3$ system, two spin transitions of Co^{3+} ions were observed at low temperatures in the concentration range $x = 0\text{-}0.3$ [6]. The $Pr_{0.5}Ca_{0.5}CoO_3$ material also exhibits a metal-insulator transition with the first-order spin-state transition. The electronic configuration of this phase at low temperature corresponds to Co^{3+} ions in ground state $t_{6(2g)}$ and Co^{4+} in intermediate-spin state $t_{5(2g)}$ [7]. This finding has revealed that Ca affects the magnetism and the charge dynamics of *Co-3d* electrons and has evoked changes in magnetic-electronic properties in the system [8].

Besides this, recent works analyzed electronic structure calculations of a ground state in the $BaCoO_3$ long-range ferromagnetic properties [9]. Several studies on cobaltite-type materials showed a metal-insulator transition associated with changes in the spin state of cobalt ions. Recent studies conclude that in the low-temperature regime of the magnetic phase of $BaCoO_3$, a two-dimensional long-range ordering is present [10].

2. Methods

Polycrystalline samples of $Ba_{1-x}Na_xCoO_3$ ($x = 0.25, 0.5, 0.75$) were prepared using a conventional solid-state reaction method from stoichiometric calculations. Appropriate amounts of stoichiometric mixtures of Na_2O_2 (99.99%), $BaCO_3$ (99.8%), and Co_3O_4 (99.99%) precursor oxides were mixed in an agate mortar for two hours. The mixture was calcined at 620 °C for fifteen hours and subsequently sintered into pellets at 640 °C for 50 hours, of which 30 hours had oxygen supply. The structural characterization by X-ray diffraction was performed using a commercial X-ray diffractometer with *Cu Kα* radiation $\lambda = 1.5405$Å in Bragg-Brentano configuration [11].

The diffraction angle was set in the $20° \leq 2\theta \leq 90°$ range, with a step size of 0.02° and two seconds per point. The diffraction patterns were refined through the Rietveld method using the GSAS program, with graphic interface EXPGUI. Magnetization was measured through an MPMS SQUID magnetometer, under temperature ranging between 5 *K* and *300 K*, and an applied magnetic field up to *5 kOe*. Magnetization as a temperature M(T) function was performed under the ZFC (zero-field cooling) procedure, in a temperature range between *5-300 K* and under a magnetic field of *50 kOe*. Magnetization concerning the applied field was measured with magnetic fields of *5 kOe*. On the other hand, the resistivity was measured with an ARS cryocooler, which can operate between *20 K* and *300 K*. The four-point method was used. A sinusoidal electrical current with an amplitude of *0.5 mA* and frequency of *37 Hz* was applied.

3. Results and discussion

3.1. Structural analysis

Figure 1 shows the XRD collected patterns of the $Ba_{1-x}Na_xCoO_3$ (x = *0.25, 0.5, 0.75*) system. The samples showed similar diffraction patterns. However, the sample with the lowest sodium concentration (x = *0.25*) showed additional diffraction peaks (*), which are associated with a second phase of Co_3O_4 (9 %). This behavior has been observed in systems with $La_{1-x}Ba_xCoO_3$ stoichiometry, where structural transitions have been reported [12].

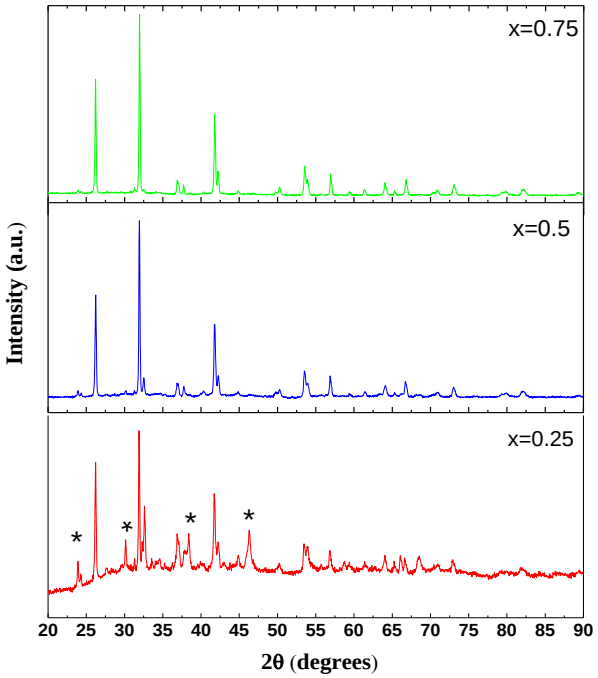

Figure 1. XRD patterns of the $Ba_{1-x}Na_xCoO_3$ system (x = *0.25, 0.5, 0.75*).

Rietveld refinement of the XRD pattern for the sample $Ba_{0.25}Na_{0.75}CoO_3$ (x = *0.75*) is shown in Figure 2. Here, the red line is the theoretical pattern. The crosses represent the experimental diffractogram, the green line represents the background, and the blue line is the difference between the experimental and the theoretical patterns. The lattice parameters, obtained via Rietveld refinement, are listed in Table 1. The Rietveld refinement analysis made it possible to identify an orthorhombic-type polycrystalline system with a majority phase of space group C_{2221} (N° 20). Figure 3 shows lattice parameters *a*, *b* and *c* as a function of sodium concentration. The lattice parameter *a* seems to be proportional to the sodium concentration increase.

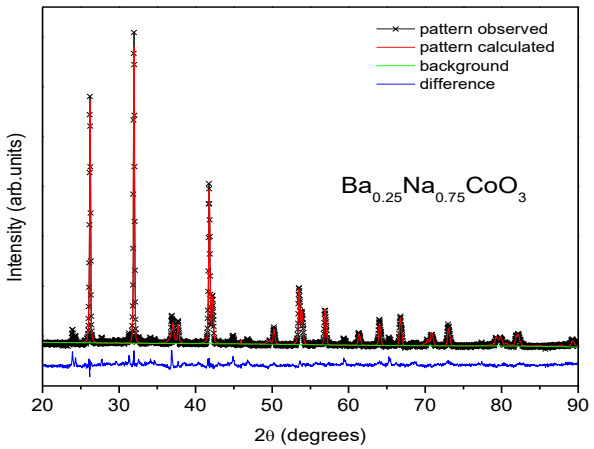

Figure 2. Rietveld refinement of the XRD pattern for the $Ba_{0.25}Na_{0.75}CoO_3$ sample.

On the other hand, the *c* lattice parameter remains constant until x = 0.5, followed by an abrupt decrease in the highest sodium concentration. This sudden change in this parameter is associated with a distortion in the crystal structure.

Table 1. Structural and fitting parameters for the main crystalline phase of the $Ba_{1-x}Na_xCoO_3$ system with x = *0.25, 0.5, 0.75* obtained by Rietveld refinement

$Ba_{0.75}Na_{0.25}CoO_3$ Group (C_{2221})				**$Ba_{0.5}Na_{0.5}CoO_3$ Group (C_{2221})**				**$Ba_{0.25}Na_{0.75}CoO_3$ Group (C_{2221})**			
a = 3.56 Å, b = 5.60 Å, c = 10.98 Å Vol = 178.91 Å^3 R = 0.24 χ^2 = 2.35				*a = 4.56 Å, b = 5.60 Å, c = 10.98Å Vol = 120.81 Å^3 R = 0.28 χ^2 = 2.17*				*a = 5.60 Å, b = 4.31 Å, c = 4.86 Å Vol = 82.61 Å^3 R = 0.21 χ^2 = 2.05*			
Atomic positions				**Atomic positions**				**Atomic positions**			
Atom	*x*	*y*	*z*	**Atom**	*x*	*y*	*z*	**Atom**	*x*	*y*	*z*
Na	0.46	0.59	0.24	**Na**	0.39	0.90	0.72	**Na**	0.75	0.90	0.74
Ba	0.70	0.64	0.31	**Ba**	0.80	0.86	0.41	**Ba**	0.21	0.24	0.48
Co	1.00	0.00	0.00	**Co**	1.00	0.00	0.00	**Co**	1.00	0.00	0.00
O	0.67	0.40	0.57	**O**	0.57	0.41	0.71	**O**	0.84	0.47	0.75

Despite the dependence of parameter *c* with sodium concentration, the unit-cell volume of the samples decreased with increasing sodium content (inset Figure 3).

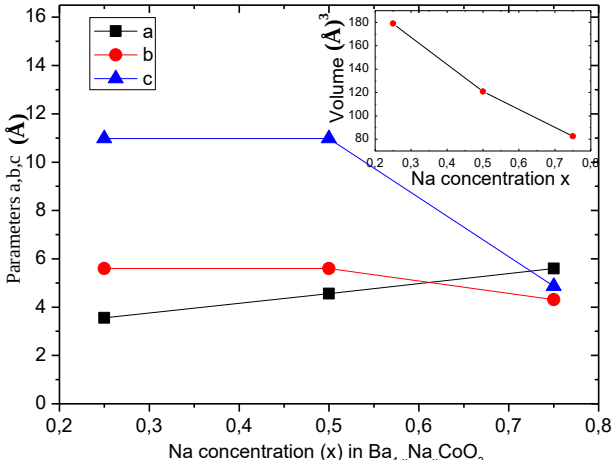

Figure 3. Lattice parameters (*a*, *b*, *c*) and unit-cell volume (inset figure) of the samples based on the sodium content.

Finally, the average crystallite size of the samples was estimated using the Scherrer formula. In all the samples, the average crystallite size was around *76 μm*. Figure 4 shows the SEM images of sodium-doped samples at *2.5 kx* magnification. The SEM images revealed the formation of porous particles with randomly oriented grains of different shapes and sizes. In particular, the microstructure for $x = 0.25$ (Figure 4a) is more homogeneous than for $x = 0.5$ and $x = 0.75$ (Figures 4b and 4c, respectively). However, a fluctuation in the size and distance between the grains as the sodium concentration changes is observable (see insert figure). The foregoing shows that the sodium concentration affects the particle size of the system under study.

3.2. Magnetic properties

The molar magnetic susceptibility measured in zero-field-cooled (ZFC) mode for $Ba_{1-x}Na_xCoO_3$, within the temperature range of *5-300 K*, is presented in Figure 5. The samples with $x = 0.5$ and $x = 0.75$ exhibited a paramagnetic behaviour. In contrast, for $x = 0.25$, the sample showed a broad maximum around *33 K*, suggesting an antiferromagnetic ordering with transition temperature Néel $T_N \approx 33$ *K*.

In a study of AC magnetization of the $BaCoO_3$ compound, Botta et al. associated this behaviour to a phase separation scenario in which a ferromagnetic region (nanoscale ferromagnetism) is immersed in a nonmagnetic matrix [13].

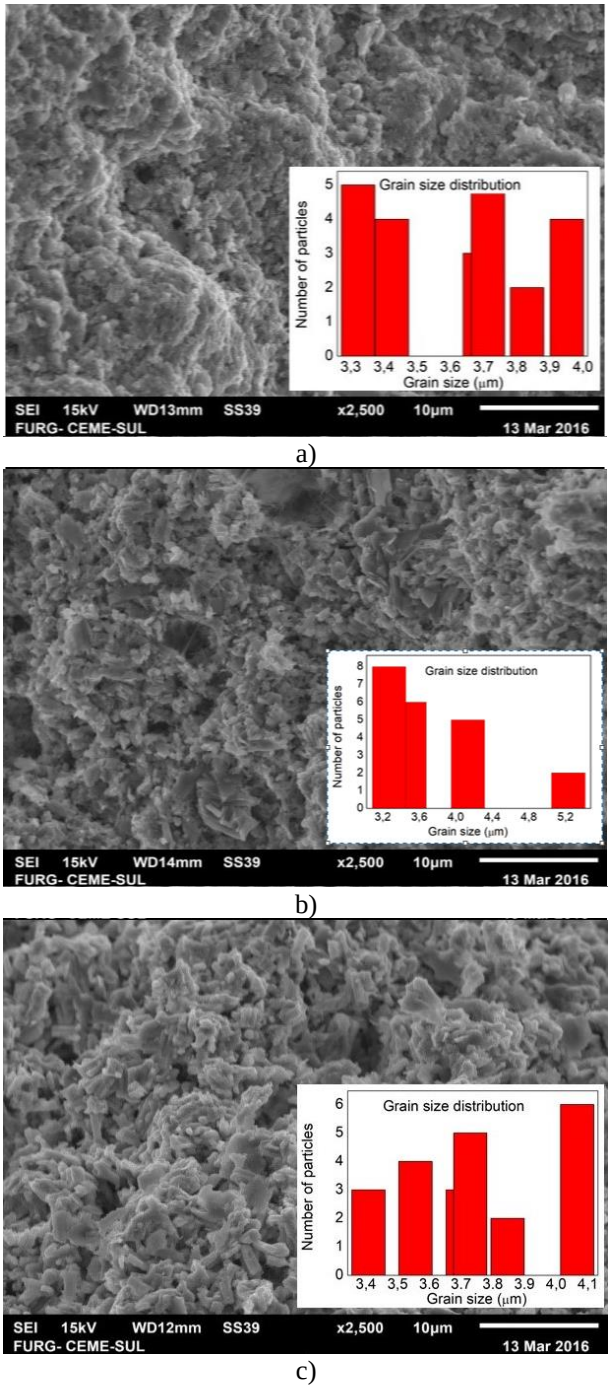

Figure 4. SEM micrographs of the $Ba_{1-x}Na_xCoO_3$ system, a) $x = 0.25$, b) $x = 0.5$, and c) $x = 0.75$.

The magnetic transition at low temperatures has also been observed in similar systems with Lanthanum and Strontium [14].

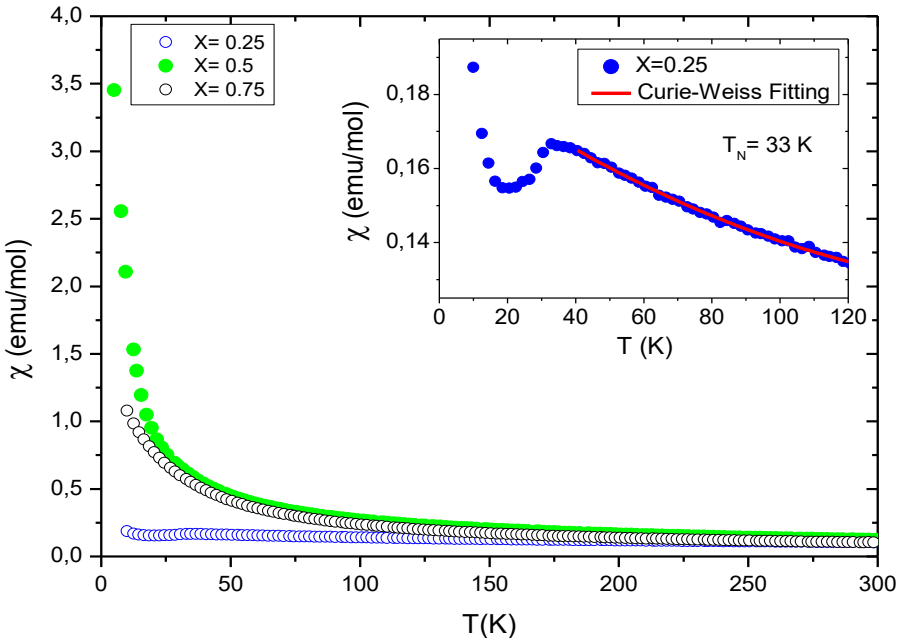

Figure 5. Thermal evolution of the $Ba_{1-x}Na_xCoO_3$ magnetic susceptibility measured under a 50 Oe magnetic field. Inset: Curie-Wiess fit for $T > 40$ K.

The inset in Figure 5 shows the best fit of the Curie-Weiss law, which may be expressed as:

$$\chi = \chi_0 + C/T - \theta, \quad (1)$$

where χ_0 is the magnetic susceptibility, θ is the Weiss constant and C is the Curie-Weiss constant which is equal to:

$$C = \mu_{eff}^2/8. \quad (2)$$

The obtained magnetic parameters are presented in Table 2. The decrease in θ with changes in the sodium content suggests that the antiferromagnetic interactions increase. Likewise, the positive theta value ($\theta > 0$) indicates spin ferromagnetic interactions. On the other hand, theoretically, the values of effective magnetic moment (μ_{eff}) are determined by equation 3.

$$\mu_{eff} = (4S(S+1))^{1/2}, \quad (3)$$

where S is the spin angular momentum of electrons [15].

If we assume that only Co^{4+} ions are in low spin ($S = 1/2$) states and contribute to the Curie constant, the existent effective magnetic moment of Co^{4+} ions are calculated to be around $1.732\ \mu_B$. Differences between the estimated value assuming a simple model and the observed ones in Table 2 are not significant. Thus, the electronic configuration of Co^{4+} ions require a complete unquenched orbital contribution for the low spin cation, which would explain the effective magnetic moments obtained by the fitted equation in the paramagnetic region of the inverse magnetic susceptibility (Figure 6).

Table 2. Calculated parameters of the Curie-Weiss equation fitting

x	C (cm^3 K/mol)	μ_{eff} (μ_B)	θ (K)	χ_0 $x10^{-4}$ (emu/o
0.75	0.48	1.96	12.17	1.56
0.5	0.37	1.72	46.24	1.39
0.25	0.43	1.85	163.23	1.16

The magnetization curves as a function of the applied field are shown in Figure 7. For samples with $x = 0.5$ and 0.75, a linear variation of the magnetization with the magnetic field was observed at all the studied temperatures with a typical characteristic of paramagnetic behavior. At $T = 5$ K, with $x = 0.25$, a small hysteresis was observed in the curve indicating a weak ferromagnetic component of magnetization with no saturation.

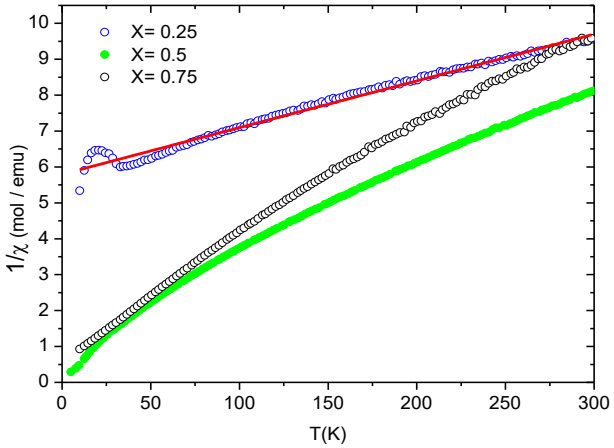

Figure 6. Inverse magnetic susceptibility as a function of temperature for the $Ba_{1-x}Na_xCoO_3$ system in the range of *5 - 300 K*

Ferromagnetic interactions were studied based on studies of similar systems by other authors. The magnitude of this ferromagnetic component is consistent with the simple cluster model, where some fraction of the Co spins exists in the nonmagnetic matrix in which the interactions are ferromagnetic [16]. In the hysteretic behavior for $x = 0.25$, a nonlinear increase in magnetization and a narrow hysteresis are observed in the low field region. The appearance of this low-temperature ferromagnetic component has also been noted in similar selenium-doped systems by previous authors [16].

3.3. Electrical properties

Figure 8 shows the temperature-dependent resistivity of the $Ba_{1-x}Na_xCoO_3$ system in the absence of an external magnetic field. For samples with $x = 0.5$ and 0.75, the electrical resistivity evidenced an insulator behaviour over the whole temperature range. However, the electrical resistivity decreased dramatically for $x = 0.5$, which indicates an increase in the carrier density. Furthermore, for the sample with $x = 0.75$, resistivity is almost independent of temperatures above ~ *280 K*.

Thus, it is reasonable to assume that the difference in the magnitude of the electrical resistivity is mainly attributed to the difference in the charge carrier density. This means that the sodium content can control the charge carrier density. In the sample with $x = 0.25$, we have observed a metal-insulator transition (inset in Figure 8). The electrical resistivity first decreases with an increase of temperature up to a typical temperature $T^* \sim 105$ *K*, indicating an insulator behaviour ($d\rho / dT < 0$). At $T > T^*$ where the resistivity increases with temperature showing a metallic behaviour ($d\rho / dT > 0$).

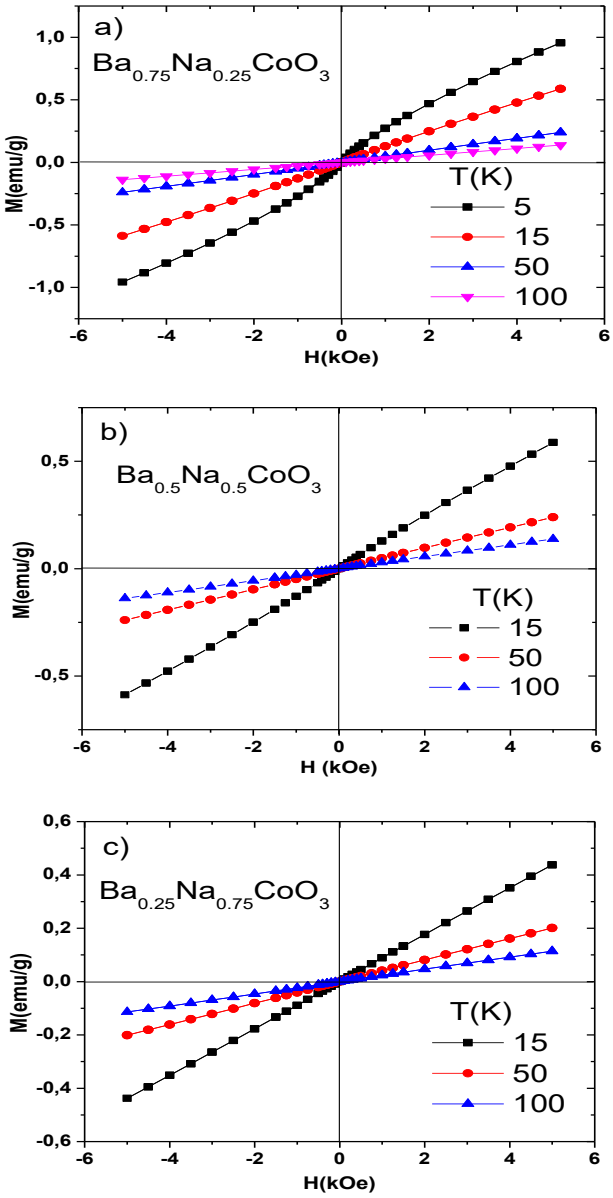

Figure 7. Magnetization loops measured as a function of the applied field at different temperatures, a) $x = 0.25$, b) $x = 0.5$, c) $x = 0.75$.

Figure 9 shows a $1/T^{-1/4}$ dependence on the resistivity for $x = 0.25$. The slope depends on the temperature. This suggests that ρ does not follow a simple activation likely due to the spin state [14], [15], [16], [17], [18]. Local activation energy E_{loc} was found to be around *3.96 meV* which is quite reasonable for this system. This value has the same order of magnitude seen in the electronic transition of $LaCoO_3$ [17]. Finally, a Ca-doped system (x = 0.2) study reported a metal-insulator transition at high temperatures in the paramagnetic state [19].

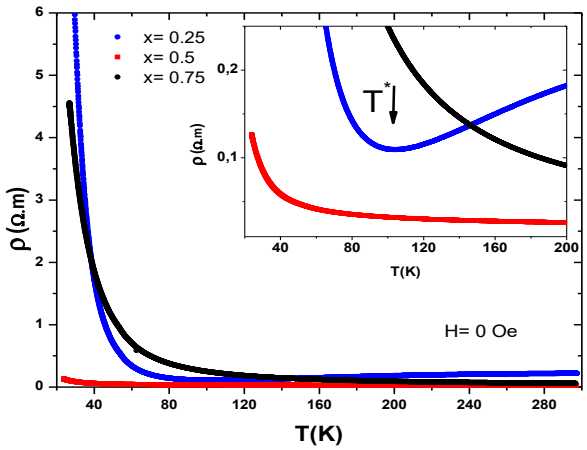

Figure 8. Resistivity as a function of temperature for the $Ba_{1-x}Na_xCoO_3$ system. The inset shows resistivity in the range *0.01-0.5 Ω.m.*

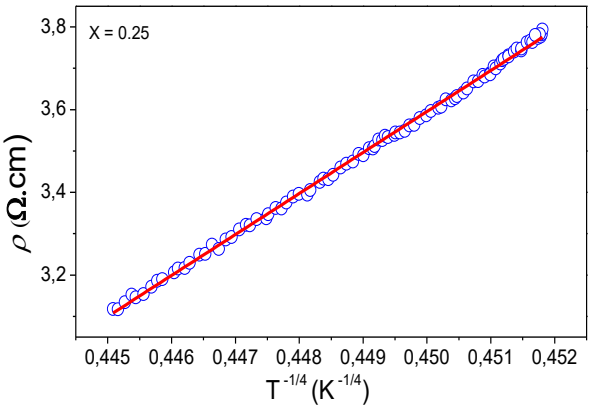

Figure 9. $T^{-1/4}$ dependence of resistivity for the $x = 0.25$ sample.

Furthermore, Kaur and Rao reported a metal-insulator transition at a temperature close to ~ 105 in epitaxial thin films [20]. Hence, the metal-insulator transition might be due to, mainly, the partial substitution of small Na (*0.95 Å*) cations by large Ba cations (*1.35 Å*).

4. Conclusion

Rietveld refinement analysis and X-ray diffraction measurements have shown that the crystal structure of $Ba_{1-x}Na_xCoO_3$ ($x = 0.25, 0.5, 0.75$) is orthorhombic with space group C_{2221} (N° 20). The sample with $x = 0.25$ exhibited a paramagnetic behavior above *33 K* due to the magnetic contribution of Co^{4+} ions in low spin configuration (LS). The susceptibility measurements evidenced the onset of an antiferromagnetic order below $T_N \approx 33$ *K*. Likewise, a weak ferromagnetic component at *5 K* was observed in the magnetization curve. The sample with $x = 0.25$ exhibited a metal-insulator transition at *105 K*, whereas the other samples presented an electrical-insulator behavior. The obtained results indicate that sodium doping at low concentration generates an antiferromagnetic behavior and metal-insulator transition in this system. These results are scientifically relevant because studying this type of material's structural, magnetic, and electrical properties contributes to expanding the application of new cobaltite materials, suggesting their potential in possible technological applications in the consumer electronics market.

Acknowledgments

Colciencias-Colombia financially supported this study through the Francisco José de Caldas Foundation (FP44842-335-2015). We acknowledge CEME-SUL / FURG for the SEM and resistivity measurements

References

[1] M. L. Foo, Y. Wang, S. Watauchi, H. W. Zandbergen, H. Tao, R. J. Cava, "Charge Ordering, Commensurability, and Metallicity in the Phase Diagram of the Layered Na_xCoO_2," *Physical review letters*, vol. 92, no. 24, pp. 247001-247004, 2004, doi: 10.1103/PhysRevLett.92.247001.

[2] G. Thornton, F. C. Morrison, S. Partington, B. C. Tofield, D. E. Williams, "The rare earth cobaltates: localised or collective electron behaviour?," *Journal of Physics C: Solid State Physics*, vol. 21, no. 15, pp. 2871, 1988, doi: 10.1088/0022-3719/21/15/019.

[3] K. Asai, A. Yoneda, O. Yokokura, J. M. Tranquada, G. Shirane, K. Kohn, "Two spin-state transitions in $LaCoO_3$," *Journal of the Physical Society of Japan*, vol. 67, no. 1, pp. 290-296, 1998, doi: 10.1143/JPSJ.67.290.

[4] Y. Ren, J. Q. Yan, J. S. Zhou, J. B. Goodenough, J. D. Jorgensen, S. Short, H. Kim, Th. Proffen, S. Chang, R. J. McQueeney, "Spin-state transitions in $PrCoO_3$ studied with neutron powder diffraction," *Physical Review B*, vol. 84, no. 21, pp. 214409, 2011, doi: 10.1103/PhysRevB.84.214409.

[5] H. Taguchi, M. Shimada, M. Koizumi, "Electrical properties in the system $(La_{1-x}Ca_x)$ CoO_3 ($0.1 \leq x \leq 0.5$)," *Journal of Solid State Chemistry*, vol. 44, no. 2, pp. 254-256, 1982, doi: 10.1016/0022-4596(82)90371-1.

[6] Y. Kobayashi, T. Mogi, K. Asai, "Spin-state transition in $La_{1-x}Pr_xCoO_3$," *Journal of the Physical Society of Japan*, vol. 75, no. 10, pp. 104703-104703, 2006, doi: 10.1143/jpsj.75.104703.

[7] S. Tsubouchi, T. Kyomen, M. Itoh, P. Ganguly, M. Oguni, Y. Shimojo, Y. Morii, "Simultaneous metal-insulator and spin-state transitions in $Pr_{0.5}Ca_{0.5}CoO_3$," *Physical Review B*, vol. 66, no. 5, pp. 052418, 2002, doi: 10.1103/PhysRevB.66.052418.

[8] K. Knižek, J. Hajtmánek, P. Novák, K. Jirák, "Charge transfer, valence, and the metal-insulator transition in $Pr_{0.5}Ca_{0.5}CoO_3$," *Physical Review B*, vol. 81, no. 15, pp. 155113, 2010, doi: 10.1103/PhysRevB.81.155113.

[9] V. Pardo, P. Blaha, M. Iglesias, K. Schwarz, D. Baldomir, J. Arias, "Magnetic structure and orbital ordering in $BaCoO_3$ from first-principles calculations," *Physical Review B*, vol. 70, no. 14, pp. 144422, 2004, doi: 10.1103/PhysRevB.70.144422.

[10] J. Sugiyama, H. Nozaki, J. H. Brewer, E. J. Ansaldo, T. Takami, H. Ikuta, "Appearance of a two-dimensional antiferromagnetic order in quasi-one-dimensional cobalt oxides," *Physical Review B*, vol. 72, no. 6, pp. 064418, 2005, doi: 10.1103/PhysRevB.72.064418.

[11] A. C. Larson, R. B. Von Dreele, "General structure analysis system (GSAS)," Los Alamos National Laboratory, New Mexico, USA, Report LAUR 86-748, 2004.

[12] W. Luo, F. Wang, "Powder X-ray diffraction and Rietveld analysis of $La_{1-x}Ca_xCoO_3$ ($0 \leq x \leq 0.5$)," *Powder diffraction*, vol. 21, no. 4, pp. 304-306, 2006, doi: 10.1154/1.2358363.

[13] P. M. Botta, V. Pardo, C. de la Calle, D. Baldomir, J. A. Alonso, J. Rivas, "Ferromagnetic clusters in polycrystalline $BaCoO_3$," *Journal of Magnetism and Magnetic Materials*, vol. 316, no. 2, pp. 670-673, 2007, doi: 10.1016/j.jmmm.2007.03.058.

[14] J. Wu, C. Leighton, "Glassy ferromagnetism and magnetic phase separation in $La_{1-x}Sr_xCoO_3$," *Physical Review B*, vol. 67, no. 17, pp. 174408, 2003, doi: 10.1103/PhysRevB.67.174408.

[15] E. Altin, E. Oz, S. Demirel, A. Bayri, "Magnetic and thermoelectric properties of B-substituted $NaCoO_2$," *Applied Physics A*, vol. 119, no. 3, pp. 1187-1196, 2015, doi: 10.1007/s00339-015-9089-0.

[16] A. Muñoz, J. A. Alonso, M. J. Martínez-Lope, E. Morán, R. Escamilla, "Synthesis and study of the crystallographic and magnetic structure of Se CoO_3," *Physical Review B*, vol. 73, no. 10, pp. 104442, 2006.

[17] R. J. Radwanski, Z. Ropka, "Magnetism and electronic structure of $LaMnO_3$ and $LaCoO_3$," *Physica B: Condensed Matter*, vol. 281, pp. 507-509, 2000, doi: 10.1016/S0921-4526(99)00931-X.

[18] P. Mandal, P. Choudhury, S. K. Biswas, B. Ghosh, "Transport and magnetic properties of $La_{1-x}Ba_xCoO_3$," *Physical Review B*, vol. 70, no. 10, pp. 104407, 2004. doi: 10.1103/PhysRevB.70.104407.

[19] K. Muta, Y. Kobayashi, K. Asai, "Magnetic, Electronic Transport, and Calorimetric Investigations of $La_{1-x}Ca_xCoO_3$ in Comparison with $La_{1-x}Sr_xCoO_3$," *Journal of the Physical Society of Japan*, vol. 71, no. 11, pp. 2784-2791, 2002, doi: 10.1143/JPSJ.71.2784.

[20] D. Kaur, K. V. Rao, "Metal-insulator transition in epitaxial thin films of $BaRuO_3$," *Journal of Physics D: Applied Physics*, vol. 36, no. 2, pp. 156, 2002, doi: 10.1088/0022-3727/36/2/313.